Int. J. Communications, Network and System Sciences, **2010, 3, 711-721**
doi:10.4236/ijcns.2010.39095 Published Online September 2010 (http://www.SciRP.org/journal/ijcns)

Scientific Research

A Virtual Channel-Based Approach to Compensation of I/Q Imbalances in MIMO-OFDM Systems

Shichuan Ma, Deborah D. Duran, Hamid Sharif, Yaoqing (Lamar) Yang
Department of Computer and Electronics Engineering, University of Nebraska-Lincoln, Omaha, USA
E-mail: *sma@huskers.unl.edu, dduran@mail.unomaha.edu, yyang3@unl.edu, hsharif@unl.edu*
Received June 28, 2010; *revised July* 28, 2010; *accepted September* 2, 2010

Abstract

Multiple-input multiple-output (MIMO)-orthogonal frequency-division multiplexing (OFDM) scheme has been considered as the most promising physical-layer architecture for the future wireless systems to provide high-speed communications. However, the performance of the MIMO-OFDM system may be degraded by in-phase/quadrature-phase (I/Q) imbalances caused by component imperfections in the analog front-ends of the transceivers. I/Q imbalances result in inter-carrier interference (ICI) in OFDM systems and cause inaccurate estimate of the channel state information (CSI), which is essential for diversity combining at the MIMO receiver. In this paper, we propose a novel approach to analyzing a MIMO-OFDM wireless communication system with I/Q imbalances over multi-path fading channels. A virtual channel is proposed as the combination of multi-path fading channel effects and I/Q imbalances at the transmitter and receiver. Based on this new approach, the effects of the channel and I/Q imbalances can be jointly estimated, and the influence of channel estimation error due to I/Q imbalances can be greatly reduced. An optimal minimal mean square error (MMSE) estimator and a low-complexity least square (LS) estimator are employed to estimate the joint coefficients of the virtual channel, which are then used to equalize the distorted signals. System performance is theoretically analyzed and verified by simulation experiments under different system configurations. The results show that the proposed method can significantly improve system performance that is close to the ideal case in which I/Q are balanced and the channel state information is known at the receiver.

Keywords: I/Q Imbalance, Multiple-Input Multiple-Output (MIMO), Orthogonal Frequency-Division Multiplexing (OFDM), Alamouti Scheme

1. Introduction

Due to the rapid growth of broadband wireless applications, the next generation of wireless communication systems poses major challenges for efficient exploitation of the available spectral resources. Among the existing techniques, the combination of orthogonal frequency-division multiplexing (OFDM) and multiple-input multiple-output (MIMO) has been widely considered the most promising approach for building future wireless transmission systems [1]. OFDM, as a popular modulation scheme, converts a frequency-selective fading channel into a parallel collection of flat-fading sub-channels, enabling high data-rate transmissions [2-4]. On the other hand, by deploying multiple antennas at both ends of the transmitter (TX) and receiver (RX), MIMO architectures are capable of combating channel fading by taking advantage of the spatial diversity and/or efficient in enhancing system capacity by employing spatial multiplexing [5,6]. The MIMO-OFDM technique has attracted significant research interest in recent years [7-10] and has been standardized in a number of communication systems [11-13].

Although OFDM presents numerous advantages, it suffers from performance degradations due to the hardware component flaws in the analog front-ends of the transceivers, including phase noise [14], carrier frequency offset [15], and in-phase/quadrature-phase (I/Q) imbalance [16,17]. The imbalance between the in-phase and the quadrature-phase branches is a major factor in performance degradation. When the received radio-frequency (RF) signal is down-converted to baseband, the analog front-end imperfections cause imbalances between the I and Q branches, which introduces inter-carrier interference (ICI) and frequency-dependent distortion to the received data. This leads to a decrease in the operating signal-to-noise

ratios (SNRs) and low data rates. Although several methods were proposed to overcome ICI [18-20], I/Q imbalances cannot be handled using these methods. The I/Q imbalances become more severe when a direct-conversion receiver (DCR) [21] or lower intermediate frequency (IF) [22] is utilized. Furthermore, the effect of the I/Q imbalances on the system is mixed with the signal distortion from the fading channel, making it difficult to compensate. Consequently, estimation and equalization of the I/Q imbalances from the received data are critical in OFDM-based systems. Frequency-independent and frequency-dependent I/Q imbalance models are reported in [16] and [17], respectively. Based on these models, the effects of I/Q imbalances are studied in OFDM systems [23-28] and in MIMO-OFDM systems [29-33].

In [29], the input-output relation of a MIMO-OFDM system with frequency-independent I/Q imbalances at the receiver is derived. Based on this result, an adaptive method is introduced to compensate for the received data. In [31], the effect of frequency-dependent I/Q imbalances on MIMO-OFDM system is studied, using a pilot-based compensation scheme. In both studies, however, the received signals are diversity combined using inaccurate channel state information (CSI) estimated under I/Q imbalances, leading to system performance degradation. We have proposed a method to deal with this problem in [33]. By jointly estimating and compensating for multi-path fading channels and I/Q imbalances, this method can effectively mitigate the I/Q effects.

In this paper, a novel approach is proposed to analyze MIMO-OFDM wireless communication systems with I/Q imbalances over multi-path fading channels. A *virtual channel* is proposed to bypass the channel estimation under I/Q influence. Based on this approach, the TX and RX I/Q imbalances are treated as parts of the fading channels. The effects of both the fading channels and I/Q imbalances on the system can be jointly estimated before diversity combining and are then employed for diversity combining and signal compensation. A minimum mean square error (MMSE) estimator and a least square (LS) estimator are used to estimate the joint coefficients of the virtual channel. A signal compensation approach based on a zero-forcing algorithm is also provided. The system performance is theoretically analyzed, and bit error rate (BER) is expressed in closed-form. Extensive simulation results verified that the I/Q imbalances at both transmitter and receiver sides can be effectively mitigated by using the virtual channel approach.

The rest of this paper is organized as follows. In the following section, a frequency-dependent I/Q imbalances model and an Alamouti scheme-based MIMO-OFDM model with transmitter and receiver I/Q imbalances are described. The input-output relation is derived in the frequency domain. In Section 3, the MMSE and LS estimators of the joint coefficients of the virtual channel are developed. In Section 4, the BER of the system is theoretically analyzed. Simulation results are given in Section 5. Finally, Section 6 concludes the paper.

Notations: A small (capital) letter represents a variable in time (frequency) domain, and a bold small (capital) letter represents a vector (matrix). The superscripts *, T, H represent the conjugate, the transpose, and the Hermitian transpose operations, respectively. $|\cdot|$ denotes absolute value operation, $\|\cdot\|$ denotes Frobenius norm, and $\varepsilon\{\cdot\}$ represents expectation. $Q(\cdot)$ represents the Q-function. $\otimes$ denotes convolution.

2. System Model

2.1. I/Q Imbalance Model

A frequency-dependent I/Q model at the receiver side is shown in **Figure 1**. As described in [17], the I/Q imbalances arise from two effects. One is the effect of the quadrature demodulator, which is frequency-independent and determined by I/Q amplitude imbalance g_{RX} and I/Q phase imbalance θ_{RX}; another is the effect of branch components, which is frequency-dependent and modeled as two filters with frequency response $L_{I,RX}(f)$ and $L_{Q,RX}(f)$. If the I/Q branches are perfect, then $g_{RX}=1$, $\theta_{RX}=0$, and $L_{I,RX}(f)=L_{Q,RX}(f)\equiv 1$.

Assuming $r_{BB}(t)$ is the baseband equivalent signal of the received signal $r_{RX}(t)$, the down-converted signal $z_{RX}(t)$ can be written as

$$z_{RX}(t)=g_{1,RX}(t)\otimes r_{BB}(t)+g_{2,RX}(t)\otimes r_{BB}^{*}(t) \quad (1)$$

where

$$\begin{aligned} g_{1,RX}(t) &= \left[l_{I,RX}(t)+l_{Q,RX}(t)g_{RX}e^{-j\theta_{RX}}\right]/2 \\ g_{2,RX}(t) &= \left[l_{I,RX}(t)-l_{Q,RX}(t)g_{RX}e^{j\theta_{RX}}\right]/2 \end{aligned} \quad (2)$$

$l_{I,RX}(t)$ and $l_{Q,RX}(t)$ are the time-domain representations of $L_{I,RX}(f)$ and $L_{Q,RX}(f)$, respectively. From the point of view of the frequency domain, the expression in (1) can be written as

$$Z_{RX}(f)=G_{1,RX}(f)R_{BB}(f)+G_{2,RX}(f)R_{BB}^{*}(-f) \quad (3)$$

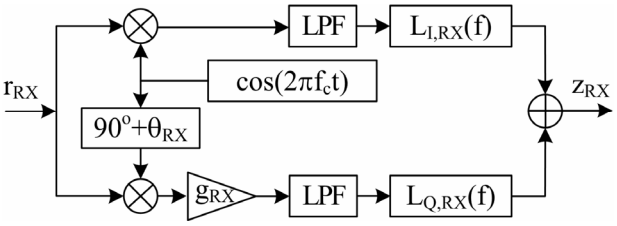

Figure 1. Block diagram of frequency-dependent I/Q imbalance at a receiver.

where $R_{BB}(f)$ is the Fourier transform of $r_{BB}(t)$, and

$$\begin{aligned} G_{1,RX}(f) &= \left[L_{I,RX}(f)+L_{Q,RX}(f)g_{RX}e^{-j\theta_{RX}}\right]/2 \\ G_{2,RX}(f) &= \left[L_{I,RX}(f)-L_{Q,RX}(f)g_{RX}e^{j\theta_{RX}}\right]/2 \end{aligned} \quad (4)$$

In (3), the term $R^*_{BB}(-f)$ represents the inter-carrier interference (ICI) projected from the mirror frequency to the signal frequency. This is called image projection, a major problem caused by I/Q imbalances in signal demodulations.

Similarly, the relation between the signal R_{TX} and the transmitted baseband signal Z_{TX} with I/Q mismatch can be written as

$$Z_{TX}(f) = G_{1,TX}(f)R_{TX}(f) + G_{2,TX}(f)R^*_{TX}(-f) \quad (5)$$

where

$$\begin{aligned} G_{1,TX}(f) &= \left[L_{I,TX}(f)+L_{Q,TX}(f)g_{TX}e^{j\theta_{TX}}\right]/2 \\ G_{2,TX}(f) &= \left[L_{I,TX}(f)-L_{Q,TX}(f)g_{TX}e^{-j\theta_{TX}}\right]/2 \end{aligned} \quad (6)$$

where g_{TX} denotes the I/Q amplitude imbalance at TX, θ_{TX} represents the I/Q phase imbalance at TX, and $L_{I,TX}(f)$ and $L_{Q,TX}(f)$ indicate the non-linear frequency characteristics of the I and Q branches at TX.

2.2. MIMO-OFDM Model with I/Q Imbalances

A block diagram of a MIMO-OFDM wireless communication system with Alamouti diversity scheme and frequency-dependent TX and RX I/Q imbalances is shown in **Figure 2**. In this system, there are two transmit antennas and N_r (≥ 1) receive antennas. All signals are represented in the form of space-time coded (STC) blocks in the frequency domain. For example, $S_{i,1} \mid S_{i,2}$ denotes an STC block data of $N \times 2$ matrix, where $i = 1, 2, \cdots$ is the STC block index, and N is the number of the used OFDM sub-carriers. Vector $\mathbf{s}_{i,j} = [S_{i,j}(-N/2)\cdots S_{i,j}(-1)\, S_{i,j}(1)\cdots S_{i,j}(N/2)]^T$ is an OFDM symbol to be transmitted over the system at the jth, $j \in \{1, 2\}$ time slot of the ith STC block, where $S_{i,j}(k)$ denotes the symbol at the kth, $k \in \{-N/2, \cdots, -1, 1, \cdots, N/2\}$ sub-carrier with average symbol energy $E_s/2$. Vector $S_{i,1}$ is transmitted followed by vector $S_{i,2}$. For simplicity, the block index i is omitted in **Figure 2**. $H_{n,m}$ denotes the channel frequency response between the nth transmit antenna and the mth receive antenna, where $n \in \{1, 2\}$ and $m \in \{1, 2, \cdots, N_r\}$. The TX I/Q imbalance parameters are denoted by $G^{(n)}_{1,TX}$ and $G^{(n)}_{2,TX}$, and the RX I/Q imbalance parameters are denoted by $G^{(m)}_{1,RX}$ and $G^{(m)}_{2,RX}$, where again, $n \in \{1, 2\}$ and $m \in \{1, 2, \cdots, N_r\}$.

Assume two consecutive data symbols, $S_{i,1}(k)$ and $S_{i,2}(k)$, to be transmitted over the kth sub-carrier. Based

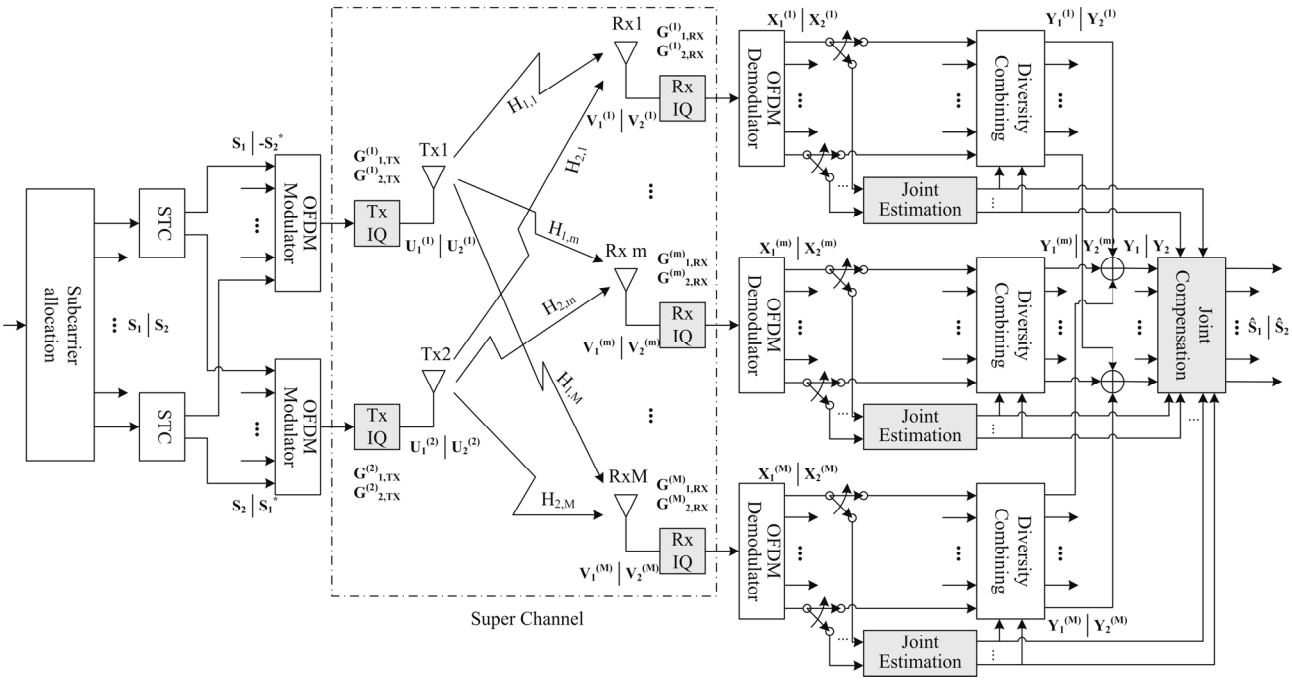

Figure 2. Block diagram of a 2×N_r MIMO-OFDM wireless communication system with transmitter and receiver I/Q imbalances. The virtual channel is illustrated in the dashed block.

on the Alamouti scheme, $S_{i,1}(k)$ and $-S_{i,2}^{*}(k)$ are distributed into the *k*th sub-carrier data stream of the first OFDM modulator, while $S_{i,2}(k)$ and $S_{i,1}^{*}(k)$ are distributed into the *k*th sub-carrier data stream of the second OFDM modulator. Data streams at all sub-carriers are then processed through OFDM modulation, including operations of padding zeros, inverse fast Fourier transform (IFFT), and adding cyclic prefix (CP). Because the IFFT operation only transforms the signal from frequency domain to time domain, the signals (viewed in the frequency domain) are not changed after OFDM modulation. Therefore, after OFDM modulation, the two consecutive data symbols at the *k*th sub-carrier of the first transmitter in the frequency domain are still $S_{i,1}(k)$ and $-S_{i,2}^{*}(k)$.

The OFDM-modulated signals are then distorted by TX I/Q imbalances. According to (5), the signals to be transmitted via the first transmit antenna are given by

$$\begin{aligned} U_{i,1}^{(1)}(k) &= G_{1,TX}^{(1)}(k)S_{i,1}(k) + G_{2,TX}^{(1)}(k)S_{i,1}^{*}(-k) \\ U_{i,2}^{(1)}(k) &= -G_{1,TX}^{(1)}(k)S_{i,2}^{*}(k) - G_{2,TX}^{(1)}(k)S_{i,2}(-k) \end{aligned} \tag{7}$$

Similarly, the signals to be transmitted via the second transmit antenna are

$$\begin{aligned} U_{i,1}^{(2)}(k) &= G_{1,TX}^{(2)}(k)S_{i,2}(k) + G_{2,TX}^{(2)}(k)S_{i,2}^{*}(-k) \\ U_{i,2}^{(2)}(k) &= G_{1,TX}^{(2)}(k)S_{i,1}^{*}(k) + G_{2,TX}^{(2)}(k)S_{i,1}(-k) \end{aligned} \tag{8}$$

The signals are then transmitted over a multi-path fading channel. The received signals at the *m*th receive antenna are given as

$$\begin{aligned} V_{i,1}^{(m)}(k) &= H_{1,m}(k)U_{i,1}^{(1)}(k) + H_{2,m}(k)U_{i,1}^{(2)}(k) \\ V_{i,2}^{(m)}(k) &= H_{1,m}(k)U_{i,2}^{(1)}(k) + H_{2,m}(k)U_{i,2}^{(2)}(k) \end{aligned} \tag{9}$$

The received signals at the *m*th receive antenna are further corrupted by I/Q imbalances in the *m*th receiver as follows:

$$\begin{aligned} W_{i,1}^{(m)}(k) &= G_{1,RX}^{(m)}(k)V_{i,1}^{(m)}(k) + G_{2,RX}^{(m)}(k)V_{i,1}^{*(m)}(-k) \\ W_{i,2}^{(m)}(k) &= G_{1,RX}^{(m)}(k)V_{i,2}^{(m)}(k) + G_{2,RX}^{(m)}(k)V_{i,2}^{*(m)}(-k) \end{aligned} \tag{10}$$

Assuming the noise in the system is additive white Gaussian noise (AWGN), then

$$\begin{aligned} X_{i,1}^{(m)}(k) &= W_{i,1}^{(m)}(k) + N_{i,1}^{(m)}(k) \\ X_{i,2}^{(m)}(k) &= W_{i,2}^{(m)}(k) + N_{i,2}^{(m)}(k) \end{aligned} \tag{11}$$

where $N_{i,j}^{(m)}(k)$ is independently identically distributed (i.i.d.) complex zero-mean Gaussian noise with variance N_0.

Combining (7), (8), (9), (10) and (11), the received data symbols at the *m*th receive antenna before diversity combining can be written as

$$\begin{aligned} X_{i,1}^{(m)}(k) &= A^{(m)}(k)S_{i,1}(k) + B^{(m)}(k)S_{i,1}^{*}(-k) + \\ &\quad C^{(m)}(k)S_{i,2}(k) + D^{(m)}(k)S_{i,2}^{*}(-k) + N_{i,1}^{(m)}(k) \\ X_{i,2}^{(m)}(k) &= C^{(m)}(k)S_{i,1}^{*}(k) + D^{(m)}(k)S_{i,1}(-k) - \\ &\quad A^{(m)}(k)S_{i,2}^{*}(k) - B^{(m)}(k)S_{i,2}(-k) + N_{i,2}^{(m)}(k) \end{aligned} \tag{12}$$

where $A^{(m)}(k)$, $B^{(m)}(k)$, $C^{(m)}(k)$, and $D^{(m)}(k)$ are defined as

$$\begin{aligned} A^{(m)}(k) &\quad G_{1,RX}^{(m)}(k)G_{1,TX}^{(1)}(k)H_{1,m}(k) + \\ &\quad G_{2,RX}^{(m)}(k)G_{2,TX}^{*(1)}(-k)H_{1,m}^{*}(-k) \\ B^{(m)}(k) &\quad G_{1,RX}^{(m)}(k)G_{2,TX}^{(1)}(k)H_{1,m}(k) + \\ &\quad G_{2,RX}^{(m)}(k)G_{1,TX}^{*(1)}(-k)H_{1,m}^{*}(-k) \\ C^{(m)}(k) &\quad G_{1,RX}^{(m)}(k)G_{1,TX}^{(2)}(k)H_{2,m}(k) + \\ &\quad G_{2,RX}^{(m)}(k)G_{2,TX}^{*(2)}(-k)H_{2,m}^{*}(-k) \\ D^{(m)}(k) &\quad G_{1,RX}^{(m)}(k)G_{2,TX}^{(2)}(k)H_{2,m}(k) + \\ &\quad G_{2,RX}^{(m)}(k)G_{1,TX}^{*(2)}(-k)H_{2,m}^{*}(-k) \end{aligned} \tag{13}$$

From (12) and (13), it is observed that the channel frequency response ($H_{n,m}$) and the I/Q effects ($G_{1,TX}^{(n)}$, $G_{2,TX}^{(n)}$, $G_{1,RX}^{(m)}$ and $G_{2,RX}^{(m)}$) are mixed together and produce the coefficients $A^{(m)}(k)$, $B^{(m)}(k)$, $C^{(m)}(k)$, and $D^{(m)}(k)$. If we treat the I/Q effects as parts of the fading channels, we can model the dashed block in **Figure 2** as a virtual channel with joint coefficients $A^{(m)}(k)$, $B^{(m)}(k)$, $C^{(m)}(k)$, and $D^{(m)}(k)$. Moreover, $A^{(m)}(k)$ and $C^{(m)}(k)$ are critical for data decoding, while the presence of $B^{(m)}(k)$ and $D^{(m)}(k)$ may introduce ICI. If the I/Q branches are perfect, then $A^{(m)}(k) = H_{1,m}(k)$, $B^{(m)}(k) = 0$, $C^{(m)}(k) = H_{2,m}(k)$, and $D^{(m)}(k) = 0$. Furthermore, the received data symbols at the *k*th sub-carrier are distorted by the mixture effects of channel and I/Q imbalances, and interference is introduced by other data symbols within the STC block at the *k*th and the mirrored -*k*th sub-carriers.

To compensate for the received signals, the joint coefficients should be estimated. The estimation methods are described in the next section. Now, assuming the accurate estimate of the joint coefficients are obtained, the received data can be combined to achieve the transmit diversity as

$$\begin{aligned} Y_{i,1}^{(m)}(k) &= A^{*(m)}(k)X_{i,1}^{(m)}(k) + C^{(m)}(k)X_{i,2}^{*(m)}(k) \\ Y_{i,2}^{(m)}(k) &= C^{*(m)}(k)X_{i,1}^{(m)}(k) - A^{(m)}(k)X_{i,2}^{*(m)}(k) \end{aligned} \tag{14}$$

It should be noted that the combining method is slightly different from the Alamouti scheme, where channel state information is employed. In our scheme, the joint coefficients $A^{(m)}(k)$ and $C^{(m)}(k)$ are used. If the I/Q branches are perfect, (14) is reduced to the standard Alamouti diversity combining scheme as substituting (12) and (13) into (14), we obtain

$$\begin{aligned} Y_{i,1}^{(m)}(k) &= H_{1,m}^{*}(k)X_{i,1}^{(m)}(k) + H_{2,m}(k)X_{i,2}^{*(m)}(k) \\ Y_{i,2}^{(m)}(k) &= H_{2,m}^{*}(k)X_{i,1}^{(m)}(k) - H_{1,m}(k)X_{i,2}^{*(m)}(k) \end{aligned} \tag{15}$$

$$\begin{aligned} Y_{i,1}^{(m)}(k) = {} & Q_1^{(m)}(k)S_{i,1}(k) + Q_2^{(m)}(k)S_{i,1}^{*}(-k) \\ & + Q_3^{(m)}(k)S_{i,2}^{*}(-k) + \tilde{N}_{i,1}^{(m)}(k) \\ Y_{i,2}^{(m)}(k) = {} & Q_1^{(m)}(k)S_{i,2}(k) + Q_2^{*(m)}(k)S_{i,2}^{*}(-k) \\ & - Q_3^{*(m)}(k)S_{i,1}^{*}(-k) + \tilde{N}_{i,2}^{(m)}(k) \end{aligned} \tag{16}$$

where

$$\begin{aligned} Q_1^{(m)}(k) &\quad |A^{(m)}(k)|^2 + |C^{(m)}(k)|^2 \\ Q_2^{(m)}(k) &\quad A^{*(m)}(k)B^{(m)}(k) + C^{(m)}(k)D^{*(m)}(k) \\ Q_3^{(m)}(k) &\quad A^{*(m)}(k)D^{(m)}(k) - C^{(m)}(k)B^{*(m)}(k) \end{aligned} \tag{17}$$

and

$$\begin{aligned} \tilde{N}_{i,1}^{(m)}(k) &= A^{*(m)}(k)n_{i,1}^{(m)}(k) + C^{(m)}(k)n_{i,2}^{*(m)}(k) \\ \tilde{N}_{i,1}^{(m)}(k) &= C^{*(m)}(k)n_{i,1}^{(m)}(k) - A^{(m)}(k)n_{i,2}^{*(m)}(k) \end{aligned} \tag{18}$$

Finally, the received data symbols at multiple receive antennas are combined to obtain receiver diversity, and the raw data symbols are given by

$$\begin{aligned} & Y_{i,1}(k) = \sum_{m=1}^{N_r}\left[Y_{i,1}^{(m)}(k)\right] = \\ & \underbrace{Q_1(k)S_{i,1}(k)}_{\text{signal}} + \underbrace{Q_2(k)S_{i,1}^{*}(-k) + Q_3^{(m)}(k)S_{i,2}^{*}(-k)}_{\text{intercarrier interference}} + \underbrace{\tilde{N}_{i,1}(k)}_{\text{noise}} \\ & Y_{i,2}(k) = \sum_{m=1}^{N_r}\left[Y_{i,2}^{(m)}(k)\right] = \\ & \underbrace{Q_1(k)S_{i,2}(k)}_{\text{signal}} + \underbrace{Q_2(k)S_{i,2}^{*}(-k) - Q_3^{*(m)}(k)S_{i,1}^{*}(-k)}_{\text{intercarrier interference}} + \underbrace{\tilde{N}_{i,2}(k)}_{\text{noise}} \end{aligned} \tag{19}$$

where

$$\begin{aligned} Q_1(k) &= \sum_{m=1}^{N_r}\left[Q_1^{(m)}(k)\right] \\ Q_2(k) &= \sum_{m=1}^{N_r}\left[Q_2^{(m)}(k)\right] \\ Q_3(k) &= \sum_{m=1}^{N_r}\left[Q_3^{(m)}(k)\right] \end{aligned} \tag{20}$$

are defined as the combined coefficients, and

$$\begin{aligned} \tilde{N}_{i,1}(k) &= \sum_{m=1}^{N_r}\left[\tilde{N}_{i,1}^{(m)}(k)\right] \\ \tilde{N}_{i,2}(k) &= \sum_{m=1}^{N_r}\left[\tilde{N}_{i,2}^{(m)}(k)\right] \end{aligned} \tag{21}$$

are the combined noise.

From (19), it can be seen that there is ICI in the signals after receiver combining, which is caused by the image projections from the mirrored frequency. To improve system performance, it is necessary to compensate for the received signals.

3. Estimators and Signal Compensation

In this section, we describe two training sequence-based estimators to show how to estimate the joint coefficients of the virtual channel. The first is a minimal mean square error (MMSE) estimator. Although MMSE estimator is an optimal linear detector, it requires some priori knowledge of the estimated variables and is computationally intensive. An alternative is a least square (LS) estimator, which may significantly reduce the computational complexity at the expense of negligible BER degradation. The estimated joint coefficients can be used to perform diversity combining as in (14) and to compensate for the received signals as described at the end of this section.

3.1. MMSE Estimator

Assume total N_{tr} blocks of training sequences are used in this system (That is $2N_{tr}$ OFDM symbols). Let $P_{i,j}(k)$, $j \in \{1,2\}$ denote the jth training symbol in the ith block at the kth sub-carrier. According to (12), the input-output relation for one block can be written as

$$\mathbf{u}_i^{(m)}(k) = \mathbf{P}_i(k)\mathbf{v}^{(m)}(k) + \mathbf{n}_i^{(m)}(k) \tag{22}$$

where

$$\mathbf{u}_i^{(m)}(k) = \left[X_{i,1}^{(m)}(k)\ X_{i,2}^{(m)}(k)\right]^T \tag{23}$$

$$\mathbf{P}_i(k) = \begin{bmatrix} P_{i,1}(k) & P_{i,1}^{*}(-k) & P_{i,2}(k) & P_{i,2}^{*}(-k) \\ -P_{i,2}^{*}(k) & -P_{i,2}(-k) & P_{i,1}^{*}(k) & P_{i,1}(-k) \end{bmatrix} \tag{24}$$

$$\mathbf{v}_i^{(m)}(k) = \left[A^{(m)}(k)\ B^{(m)}(k)\ C^{(m)}(k)\ D^{(m)}(k)\right]^T \tag{25}$$

$$\mathbf{n}_i^{(m)}(k) = \left[N_{i,1}^{(m)}(k)\ N_{i,2}^{(m)}(k)\right]^T \tag{26}$$

For the total T blocks, the input-output relation is written as

$$\mathbf{u}^{(m)}(k) = \mathbf{P}(k)\mathbf{v}^{(m)}(k) + \mathbf{n}^{(m)}(k) \tag{27}$$

where

$$\mathbf{u}^{(m)}(k) = \left[\mathbf{u}_1^{(m)}(k)^T\ \mathbf{u}_2^{(m)}(k)^T \cdots \mathbf{u}_{N_{tr}}^{(m)}(k)^T\right]^T \tag{28}$$

$$\mathbf{P}(k) = \left[\mathbf{P}_1(k)^T\ \mathbf{P}_2(k)^T \cdots \mathbf{P}_{N_{tr}}(k)^T\right] \tag{29}$$

$$\mathbf{n}^{(m)}(k) = \left[\mathbf{n}_1^{(m)}(k)^T\ \mathbf{n}_2^{(m)}(k)^T \cdots \mathbf{n}_{N_{tr}}^{(m)}(k)^T\right]^T \tag{30}$$

The MMSE estimate of $\mathbf{v}$ is given as [34]

$$\hat{\mathbf{v}}^{(m)}(k) = \mathbf{R}_{vu}\mathbf{R}_u^{-1}\mathbf{u}^{(m)}(k) \tag{31}$$

where

$$\mathbf{R}_{vu} = E\{\mathbf{v}^{(m)}(k)\mathbf{u}^{(m)}(k)^H\} = \mathbf{R}_v\mathbf{P}^H(k) \tag{32}$$

$$\mathbf{R}_u = E\{\mathbf{u}^{(m)}(k)\mathbf{u}^{(m)}(k)^H\} = \mathbf{P}(k)\mathbf{R}_v\mathbf{P}^H(k) + \mathbf{R}_n \tag{33}$$

$$\mathbf{R}_n = E\{\mathbf{n}^{(m)}(k)\mathbf{n}^{(m)}(k)^H\} = N_0\mathbf{I}_{2T} \tag{34}$$

$$\mathbf{R}_v = E\{\mathbf{v}^{(m)}(k)\mathbf{v}^{(m)}(k)^H\} \tag{35}$$

3.2. LS Estimator

Although MMSE estimator is optimal, it suffers from high computational complexity and requires the knowledge of $\mathbf{R}_v$, which must be estimated using a large amount of transmission data. A simple but effective method is least square estimator. To further reduce the computational complexity, we design a special training pattern to avoid matrix inversion operation. In order to utilize this special pattern, training sequences must be transmitted in groups of two blocks. Let s, s, s, and s^* be the four consecutive training symbols within the ith and the $(i+1)$th STC blocks at the kth sub-carrier, where $s = p(1+j)$ is a complex number with identical real and imaginary parts p. The corresponding training symbols at the $-k$th sub-carrier are also s, s, s, and s^*. According to (12), the received data within the ith and the $(i+1)$th STC blocks at the kth sub-carrier can be represented in matrix form as

$$\begin{bmatrix} X_{i,1}^{(m)}(k) \\ X_{i,2}^{(m)}(k) \\ X_{i+1,1}^{(m)}(k) \\ X_{i+1,2}^{(m)}(k) \end{bmatrix} = \begin{bmatrix} s & s^* & s & s^* \\ -s^* & -s & s^* & s \\ s & s^* & s^* & s \\ -s & -s^* & s^* & s \end{bmatrix} \mathbf{v}^{(m)}(k) + \begin{bmatrix} N_{i,1}^{(m)}(k) \\ N_{i,2}^{(m)}(k) \\ N_{i+1,1}^{(m)}(k) \\ N_{i+1,2}^{(m)}(k) \end{bmatrix} \tag{36}$$

Thus, the LS estimate of the joint coefficients is given as [35]

$$\begin{aligned} \hat{\mathbf{v}}^{(m)}(k) &= \begin{bmatrix} s & s^* & s & s^* \\ -s^* & -s & s^* & s \\ s & s^* & s^* & s \\ -s & -s^* & s^* & s \end{bmatrix}^{-1} \begin{bmatrix} X_{i,1}^{(m)}(k) \\ X_{i,2}^{(m)}(k) \\ X_{i+1,1}^{(m)}(k) \\ X_{i+1,2}^{(m)}(k) \end{bmatrix} \\ &= \frac{1}{4p} \begin{bmatrix} 0 & -1-j & 1 & j \\ 0 & -1+j & 1 & -j \\ 1-j & 0 & j & 1 \\ 1+j & 0 & -j & 1 \end{bmatrix} \begin{bmatrix} X_{i,1}^{(m)}(k) \\ X_{i,2}^{(m)}(k) \\ X_{i+1,1}^{(m)}(k) \\ X_{i+1,2}^{(m)}(k) \end{bmatrix} \end{aligned} \tag{37}$$

The estimates of the virtual channel coefficients from different training sequence groups can be averaged to obtain more accurate estimate.

3.3. Signal Compensation Approach

Based on the MMSE estimate given by (31) or LS estimate given by (37) of the joint coefficients, the estimate of the combined coefficients, $\hat{Q}_1(k)$, $\hat{Q}_2(k)$, and $\hat{Q}_3(k)$, can be calculated according to (17) and (20), and then can be used to equalize the raw data symbols. According to (19), the raw data symbols at the kth and the $(-k)$th sub-carriers within the ith STC block can be written in matrix form as (38). Thus, the zero-forcing estimates of the transmitted data symbols are given by (39).

$$\begin{bmatrix} Y_{i,1}(k) \\ Y_{i,1}^*(-k) \\ Y_{i,2}(k) \\ Y_{i,2}^*(-k) \end{bmatrix} = \begin{bmatrix} \hat{Q}_1(k) & \hat{Q}_2(k) & 0 & \hat{Q}_3(k) \\ \hat{Q}_2^*(-k) & \hat{Q}_1^*(-k) & \hat{Q}_3^*(-k) & 0 \\ 0 & -\hat{Q}_3^*(k) & \hat{Q}_1(k) & \hat{Q}_2^*(k) \\ -\hat{Q}_3(-k) & 0 & \hat{Q}_2(-k) & \hat{Q}_1^*(-k) \end{bmatrix} \begin{bmatrix} S_1(k) \\ S_1^*(-k) \\ S_2(k) \\ S_2^*(-k) \end{bmatrix} + \begin{bmatrix} \tilde{N}_{i,1}(k) \\ \tilde{N}_{i,1}(-k) \\ \tilde{N}_{i,2}(k) \\ \tilde{N}_{i,2}(-k) \end{bmatrix} \tag{38}$$

$$\begin{bmatrix} \hat{S}_1(k) \\ \hat{S}_1^*(-k) \\ \hat{S}_2(k) \\ \hat{S}_2^*(-k) \end{bmatrix} = \begin{bmatrix} \hat{Q}_1(k) & \hat{Q}_2(k) & 0 & \hat{Q}_3(k) \\ \hat{Q}_2^*(-k) & \hat{Q}_1^*(-k) & \hat{Q}_3^*(-k) & 0 \\ 0 & -\hat{Q}_3^*(k) & \hat{Q}_1(k) & \hat{Q}_2^*(k) \\ -\hat{Q}_3(-k) & 0 & \hat{Q}_2(-k) & \hat{Q}_1^*(-k) \end{bmatrix}^{-1} \begin{bmatrix} Y_{i,1}(k) \\ Y_{i,1}^*(-k) \\ Y_{i,2}(k) \\ Y_{i,2}^*(-k) \end{bmatrix} \tag{39}$$

4. Performance Analysis

According to (19), the received raw data symbols are contaminated by noise and interference from the signals at the mirrored sub-carriers. If the ICI can be successfully canceled by the proposed algorithm, the post- processing SNR at the kth sub-carrier, $\eta(k)$, can be calculated as

$$\begin{aligned} \eta(k) &= \frac{\varepsilon\left\{|\, Q_1(k) S_{i,1}(k)\,|^2\right\}}{\varepsilon\left\{|\, \tilde{n}_{i,1}(k)\,|^2\right\}} = \frac{\varepsilon\left\{|\, Q_1(k) S_{i,2}(k)\,|^2\right\}}{\varepsilon\left\{|\, \tilde{n}_{i,2}(k)\,|^2\right\}} \\ &= \sum_{m=1}^{N_r} \left[|\, A^{(m)}(k)\,|^2 + |\, C^{(m)}(k)\,|^2\right] \frac{E_s/2}{N_0} \\ &= \frac{1}{2} \sum_{m=1}^{N_r} \left[|\, A^{(m)}(k)\,|^2 + |\, C^{(m)}(k)\,|^2\right] \rho \end{aligned} \tag{40}$$

where $E_s/2$ is the average transmit energy per symbol period per antenna and $\rho = E_s / N_0$ can be interpreted as the average SNR for the single-input single-output scheme.

This post-processing SNR is determined by the joint effects of channels and I/Q imbalances. For classical i.i.d. channels [5] and perfect I/Q characteristics, the post-processing SNR becomes

$$\eta(k) = N_r \rho \tag{41}$$

This shows that the system with perfect I/Q over i.i.d. channel can achieve an array gain of N_r.

In OFDM systems, each sub-carrier can be treated as a frequency-flat channel. Assuming optimum detection at the receiver, the corresponding symbol error rate for rectangular M-ary QAM is given by [36]

$$P_s(k) = 1 - \left(1 - 2\left(1 - \frac{1}{\sqrt{M}}\right) Q\left(\sqrt{\frac{3\eta(k)}{M-1}}\right)\right)^2 \quad (42)$$

Assuming that only one single bit is changed for each erroneous symbol, the equivalent bit error rate for rectangular M-ary QAM is approximated as [37]

$$P_b(k) \approx \frac{1}{log_2(M)} P_s(k) \quad (43)$$

5. Simulation Results

To evaluate the proposed virtual channel idea, the two estimators, and the signal compensation approach, we used MATLAB to simulate an OFDM-based $2 \times N_r$ MIMO system with frequency-dependent TX and RX I/Q imbalances. The size of fast Fourier transform (FFT) is 128, the number of used sub-carriers is 96, and the length of CP is 32. The multi-path channel is modeled by six independent complex taps with a power delay profile of a 3 dB decay per tap. It should be noted that the actual channel length can be estimated [38]. The simulation bandwidth is set to 20 MHz, leading to a 156.25 KHz sub-carrier spacing and a maximum 0.3 μs excess delay. Sixty-four quadrature amplitude modulations (64QAM) are used.

The non-linear frequency characteristics of the I and Q branches, $L_I(f)$ and $L_Q(f)$, are modeled as two first-order finite impulse response (FIR) filters. A form of parameters $\{g, \theta, [a_I, b_I], [a_Q, b_Q]\}$ is used to describe the I/Q imbalance, where $[a_I, b_I]$ and $[a_Q, b_Q]$ are the coefficients of the FIR filters for the I and Q branches. I/Q parameters of $\{1.03, 3, [0.01, 0.9], [0.8, 0.02]\}$ and $\{[0.8, 0.02], [0.01, 0.9]\}$ are used for the two transmitters, respectively. For simplification of simulation, all receivers use I/Q parameters of $\{1.05, 3, [0.8, 0.02], [0.9, 0.01]\}$. Because the estimation of the joint coefficients is performed separately in each receiver, the same I/Q parameters for different I/Q models still lead to generalization of the simulation results. It should be noted that the I/Q imbalance parameters are chosen to be worst case in order to evaluate the robustness of the proposed approach.

A frame-by-frame transmission scheme is employed in the simulation. The multi-path channel is independently generated for each frame. One frame consists of N_{tr} STC blocks of training symbols followed by 50 STC blocks of data symbols. A total of 5,000 frames (288 Mbits) are simulated for each scenario at a given SNR.

Figure 3 shows the frequency response of two of the FIR filters used for simulating the frequency-dependent characteristics of I/Q imbalances. For both filters, the variations of the amplitude are within 0.5 dB, but the average gains are differentiated by 1 dB. It should be noted that the signals after TX I/Q distortions must be normalized in the simulations to compensate for the energy lost due to attenuations of the filters. While the variation of the phase response for the first filter is small, the variation is very large for the second filter. The amplitude and phase differences of the filters are suitable to simulate the frequency-dependent characteristics of I/Q imbalances.

Figure 4 shows the typical constellations of one frame of symbols generated in an ideal channel environment (without multi-path fading and noise). **Figures 4** (a) and (b) show the constellations of the raw data symbols under frequency-independent and frequency-dependent I/Q imbalances, respectively. It is observed that the constellation in **Figure 4** (b) becomes nearly random compared with **Figure 4** (a) due to the effect of frequency-de pendent I/Q imbalances. **Figure 4** (c) shows the constellation of signals recovered by the proposed LS algorithm, which shows that the proposed algorithm can perfectly compensate frequency-independent and frequency-dependent I/Q imbalances.

The BER performances of the proposed estimators and compensation approach are shown in **Figures 5-10**. To make better comparisons, a series of simulations under different scenarios was conducted, including a scenario of perfect I/Q and CSI known at receivers termed as "ideal case", a scenario with frequency-independent I/Q imbalances termed as "indep-IQ", and a scenario with frequency-dependent I/Q imbalances termed as "dep-IQ". The legend term of "NoComp" means that I/Q imbalances are present but no compensation scheme is applied (the CSI is estimated under I/Q imbalances), "MMSE (N)" means that the MMSE estimator with N STC blocks of training sequences (the total $2 \times N$ OFDM

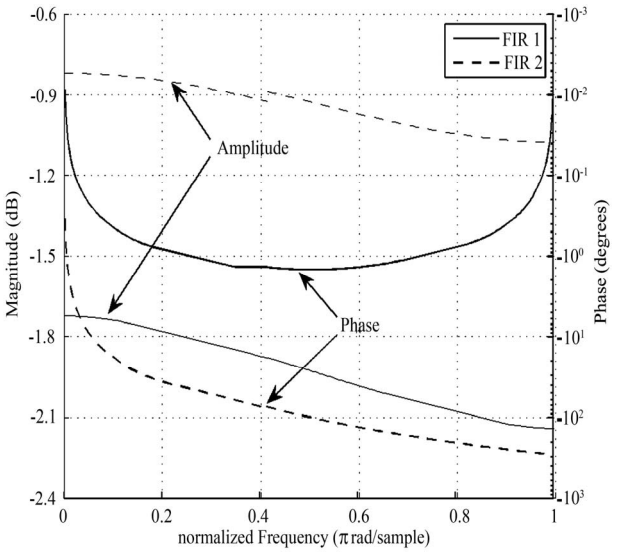

Figure 3. Frequency response of the FIR filters used for simulating the frequency-dependent characteristics of I/Q imbalances; coefficients of FIR 1 are [0.8, 0.02], and coefficients for FIR 2 are [0.01,0.9].

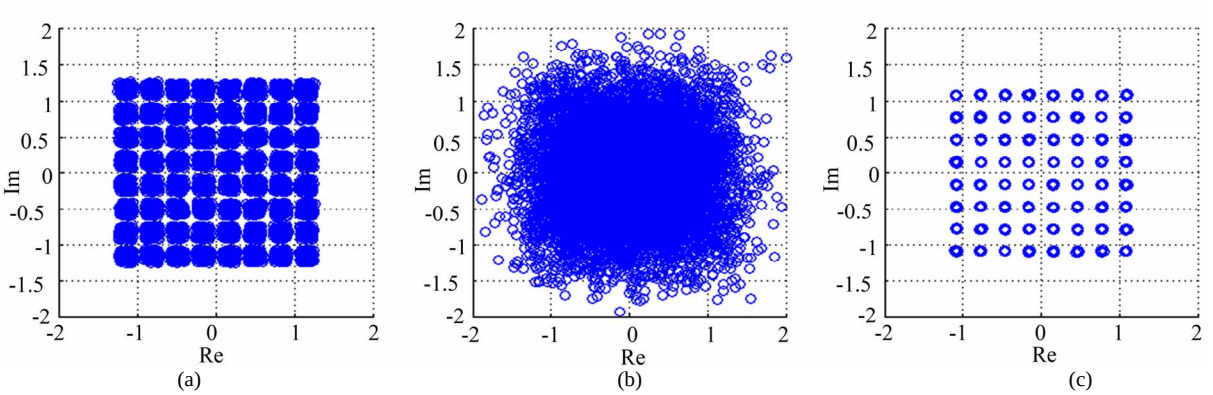

Figure 4. Constellations of signals in a frame generated by a 2 × 1 MIMO-OFDM system under ideal channel environment. (a) raw data constellations under frequency-independent I/Q imbalances; (b) raw data constellations under frequency-dependent I/Q imbalances; (c) constellations of the compensated data under frequency-dependent I/Q imbalances.

symbols) is used, and "LS(N)" means that the LS estimator with N STC blocks of training sequence is used to estimate the joint coefficients. For both MMSE and LS estimators, the proposed compensation approach is applied to compensate the received raw data symbols. Furthermore, the BER is theoretically calculated according to (43) and is shown in the following figures with legend term "analysis".

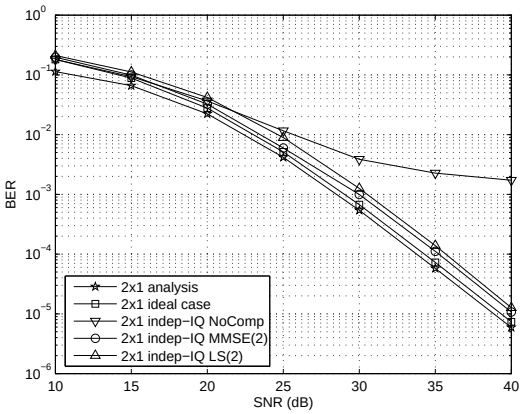

Figure 5. Performance of a 2 × 1 MIMO-OFDM system with TX and RX frequency-independent I/Q imbalances over multi-path fading channel.

Figure 5 and **Figure 6** show the performance of a 2×1 and a 2×2 systems with frequency-independent I/Q imbalances, respectively. It is observed from the "Nocomp" curves that the I/Q imbalances significantly degrade the system performance, resulting in high error floor. These results agree with the constellation analysis mentioned above. With the proposed estimators and signal compensation approach, the I/Q distortion can be effectively mitigated and the system performance is significantly improved. By using two STC blocks of training sequences, the system performance resulting from both MMSE and LS estimators is close to the ideal case. The performance degradation is less than 1 dB. Although LS estimator performs a little worse than MMSE estimator, the low computational complexity makes the LS estimator more competitive. By assuming perfect estimation of the

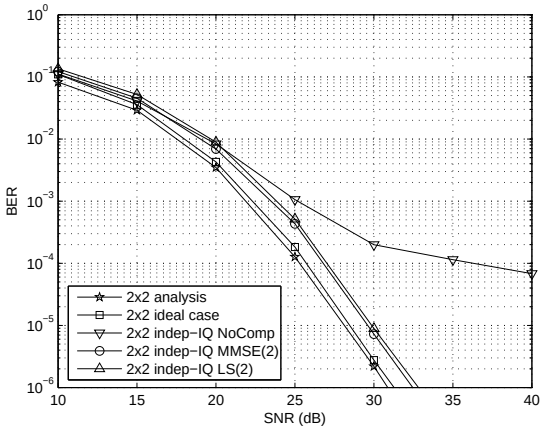

Figure 6. Performance of a 2 × 2 MIMO-OFDM system with TX and RX frequency-independent I/Q imbalances over multi-path fading channel.

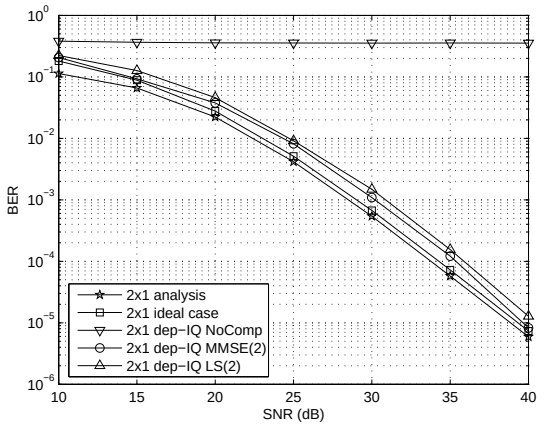

Figure 7. Performance of a 2 × 1 MIMO-OFDM system with TX and RX frequency-dependent I/Q imbalances over multi-path fading channel.

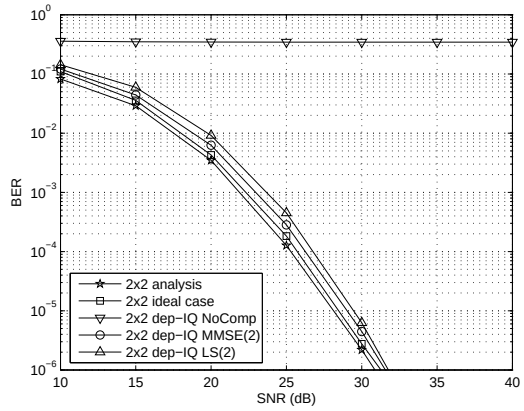

Figure 8. Performance of a 2 × 2 MIMO-OFDM system with TX and RX frequency-dependent I/Q imbalances over multi-path fading channel.

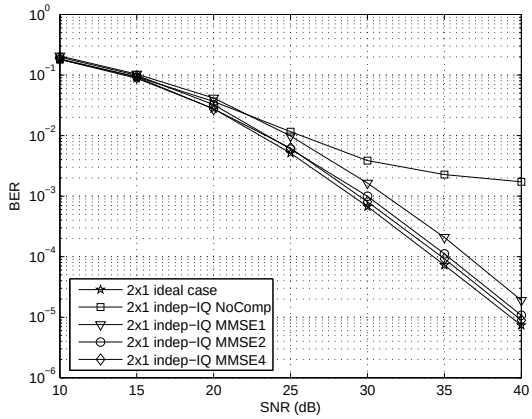

Figure 9. Comparison of the performances of the MMSE estimator with different lengths of training symbols for the 2 × 1 MIMO-OFDM system with TX and RX frequency-independent I/Q imbalances over multi-path fading channel.

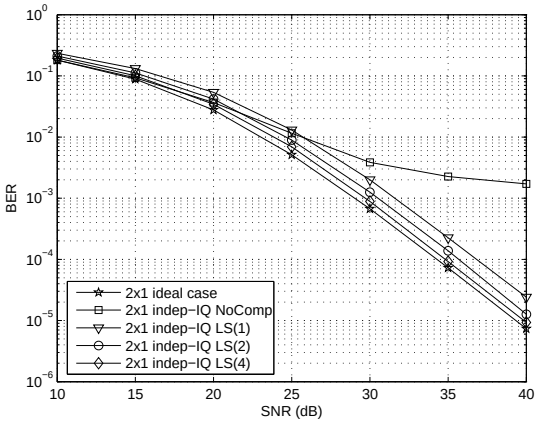

Figure 10. Comparison of the performances of the LS estimator with different lengths of training symbols for the 2 × 1 MIMO-OFDM system with TX and RX frequency-independent I/Q imbalances over multi-path fading channel.

joint coefficients and compensation of the received signal, it is reasonable that the analysis results are slightly better than the ideal case.

The performance of the systems with frequency-dependent I/Q imbalances are shown in **Figure 7** and **Figure 8** for the 2×1 and 2×2 scenarios, respectively. The frequency dependent characteristic of the I/Q imbalances causes fatal influence on the MIMO-OFDM systems. Without compensation, the BER remains one half regardless of the SNR. Our proposed approach can also successfully combat the worst fading effect caused by frequency-dependent I/Q imbalances, resulting in good performance that is close to the ideal case. This significant performance improvement has not been reported by other literatures.

An intuitive sense is that a longer training sequence could result in better performance. To demonstrate this point, we compare the system performances with different lengths of training symbols in **Figure 9** and **Figure 10** for MMSE and LS estimators, respectively. It is observed that BER decreases with the increase of the training symbol numbers. When four blocks of training sequences are used, the performance loss compared to the ideal case is negligible.

6. Conclusions

In this paper, we introduce a new virtual channel concept to analyze the I/Q imbalances in a MIMO-OFDM wireless communication system over multi-path fading channels. The input-output relation is derived in frequency domain, which incorporates the effect of I/Q imbalances with multi-path fading channels. The integrated effect can be modeled by the joint coefficients of the virtual channel. By using this approach, inaccurate estimation of the channel state information can be avoided at the diversity combining stage. The joint coefficients are estimated by using the proposed MMSE and LS estimators, and are used to compensate the received signals. Simulation results show that the proposed approach can effectively mitigate the TX and RX I/Q imbalances in MIMO-OFDM systems. Although only a two transmit antenna scheme is illustrated in this paper, our proposed approach can be easily extended to any number of transmit antenna configurations by using orthogonal space-time block coding.

7. Acknowledgements

This study was supported by the Advanced Telecommunications Engineering Laboratory (www.TEL.unl.edu) and was partially funded by the US Federal Railroad Administration (FRA) under the direction of Terry Tse.

8. References

[1] M. Jang and L. Hanzo, "Multiuser MIMO-OFDM for Next-Generation Wireless Systems," *Proceedings of the IEEE*, Vol. 95, No. 7, July 2007, pp. 1430-1469.

[2] R. Chang and R. Gibby, "A Theoretical Study of Performance of an Orthogonal Multiplexing Data Transmission Scheme," *IEEE Transactions on Communications Technology*, Vol. 16, No. 4, August 1968, pp. 529-540.

[3] Y. Wu and W. Y. Zou, "Orthogonal Frequency Division Multiplexing: A Multi-Carrier Modulation Scheme," *IEEE Transactions on Consumer Electronics*, Vol. 41, No. 3, August 1995, pp. 392-399.

[4] L. Hanzo, M. Muinster, B. Choi and T. Keller, "OFDM and MC-CDMA for Broadband Multi-User Communications," Wlans and Broadcasting, Wiley, 2003.

[5] A. Paulraj, R. Nabar and D. Gore, "Introduction to Space-Time Wireless Communications," Cambridge University Press, Cambridge, 2003.

[6] Y. Yang, G. Xu and H. Ling, "An Experimental Investigation of Wideband MIMO Channel Characteristics Based on Outdoor Non-Los Measurements at 1.8 GHz," *IEEE Transactions on Antennas Propagation*, Vol. 54, November, 2006, pp. 3274-3284.

[7] H. Sampath, S. Talwar, J. Tellado, V. Erceg and A. J. Paulraj, "A Fourth-Generation MIMO-OFDM Broadband Wireless System: Design, Performance and Field Trial Results," *IEEE Communications Magazine*, Vol. 40, No. 9, September 2002, pp. 143-149.

[8] G. L. St¨uber, J. R. Barry, S. W. McLaughlin, Y. G. Li, M. A. Ingram and T. G. Pratt, "Broadband MIMO-OFDM Wireless Communications," *Proceedings of the IEEE*, Vol. 92, No. 2, February 2004, pp. 271-294.

[9] Y. Li, J. H. Winters and N. R. Sollenberger, "MIMO-OFDM for Wireless Communications: Signal Detection with Enhanced Channel Estimation," *IEEE Transactions on Communications*, Vol. 50, No. 9, September, 2002, pp. 1471-1477.

[10] M. Shin, H. Lee and C. Lee, "Enhanced Channel-Estimation Technique for MIMO-OFDM Systems," *IEEE Communications Letters*, Vol. 53, No. 1, January 2004, pp. 262-265.

[11] IEEE Standard for Local and Metropolitan Area Networks, Part 16: Air Interface for Fixed Broadband Wireless Access System, October 2004.

[12] IEEE Candidate Standard 802.11n: Wireless LAN Medium Access Control (MAC) and Physical Layer (PHY) Specifications, 2004.

[13] 3GPP Technical Specification Group Radio Access Network, Overall Description of E-UTRA/E-UTRAN, 2007.

[14] S. R. Herlekar, C. Zhang, H.-C. Wu, A. Srivastava and Y. Wu, "OFDM Performance Analysis in the Phase Noise Arising from the Hot-Carrier Effect," *IEEE Transactions on Consumer Electronics*, Vol. 52, No. 3, August 2006, pp. 757-765.

[15] J. Lei and T.-S. Ng, "A Consistent OFDM Carrier Frequency Offset Estimator Based on Distinctively Spaced Pilot Tones," *IEEE Transactions on Wireless Communications*, Vol. 3, No. 2, March 2004, pp. 588-599.

[16] C. L. Liu, "Impacts of I/Q Imbalance on QPSK-OFDM-QAM Detection," *IEEE Transactions on Consumer Electronics*, Vol. 44, No. 3, August 1998, pp. 984-989.

[17] M. Valkama, M. Renfors and V. Koivunen, "Compensation of Frequency-Selective I/Q Imbalances in Wideband Receivers: Models and Algorithms," *Proceedings of the* 3*rd IEEE Workshop on Signal Processing Advances in Wireless Communications*, Taiwan, March 2001, pp. 42-45.

[18] H.-C. Wu and Y. Wu, "Distributive Pilot Arrangement Based on Modified M-sequences for OFDM Inter-Carrier Interference Estimation," *IEEE Transactions on Wireless Communications*, Vol. 6, No. 5, May 2007, pp. 1605-1609.

[19] X. Huang and H.-C. Wu, "Robust and Efficient Inter-Carrier Interference Mitigation for OFDM Systems in Time-Varying Fading Channels," *IEEE Transactions on Vehicular Technology*, Vol. 56, No. 5, September 2007, pp. 2517-2528.

[20] H.-C. Wu, X. Huang, Y. Wu and X. Wang, "Theoretical Studies and Efficient Algorithm of Semi-Blind ICI Equalization for OFDM," *IEEE Transactions on Wireless Communications*, Vol. 7, No. 10, October 2008, pp. 3791-3798.

[21] A. A. Abidi, "Direct-Conversion Radio Transceivers for Digital Communications," *IEEE Journal of Solid-State Circuits*, Vol. 30, No. 12, December 1995, pp. 1399-1410.

[22] J. Crols and M. Steyaert, "Low-IF Topologies for High-Performance Analog Front Ends of Fully Integrated Receivers," *IEEE Transactions on Circuits System*, Vol. 45, No. 3, March 1998, pp. 269-282.

[23] A. Tarighat, R. Bagheri and A. H. Sayed, "Compensation Schemes and Performance Analysis of IQ Imbalances in OFDM Receivers," *IEEE Transactions on Signal Processing*, Vol. 53, No. 8, August 2005, pp. 3257-3268.

[24] J. K. Hwang, W. M. Chen, Y. L. Chiu, S. J. Lee and J. L. Lin, "Adaptive Baseband Compensation for I/Q Imbalance and Time-Varying Channel in OFDM System," *Intelligent Signal Processing and Communications*, Japan, December 2006, pp. 638 – 641.

[25] J. Tubbax, B. Come, L. van der Perre, S. Donnay, M. Engles and C. Desset, "Joint Compensation of IQ Imbalance and Phase Noise," *IEEE Semiannual on Vehicular Technology Conference*, Vol. 3, April 2003, pp. 1605-1609.

[26] D. Tandur and M. Moonen, "Joint Compensation of OFDM Frequency-Selective Transmitter and Receiver IQ Imbalance," *EURASIP Journal on Wireless Communications and Networking*, Vol. 2007, No. 68563, May 2007, pp. 1-10.

[27] L. Anttila, M. Valkama and M. Renfors, "Frequency-Selective I/Q Mismatch Calibration of Wideband Direct-Conversion Transmitters," *IEEE Transactions on Circuits System*, Vol. 55, No. 4, April 2008, pp. 359-363.

[28] S. Ma, D. Duran and Y. Yang, "Estimation and Compen-

sation of Frequency-Dependent I/Q Imbalances in OFDM Systems over Fading Channels," *Proceedings of the* 5*th International Conference on Wireless Communications, Networking and Mobile Computing*, Beijing, September 2009.

[29] A. Tarighat, W. M. Younis and A. H. Sayed, "Adaptive MIMO OFDM Receivers: Implementation Impairments and Complexity Issues," *IFAC Workshop on Adaptation and Learning in Control and Signal Processing*, Yokohama, August 2004.

[30] Y. Zou, M. Valkama and M. Renfors, "Digital Compensation of I/Q Imbalance Effects in Space-Time Coded Transmit Diversity Systems," *IEEE Transactions on Signal Process*, Vol. 56, No. 6, June 2008, pp. 2496-2508.

[31] Y. Zou, M. Valkama and M. Renfors, "Analysis and Compensation of Transmitter and Receiver I/Q Imbalances in Space-Time Coded Multi-Antenna OFDM Systems," *EURASIP Journal on Wireless Communications and Networking*, No. 391025, January 2008, pp. 1-10.

[32] D. Tandur and M. Moonen, "Compensation of RF Impairments in MIMO OFDM Systems," *IEEE International Conference on Acoustics, Speech and Signal Processing*, Las Vegas, April 2008, pp. 3097-3100.

[33] S. Ma, D. Duran, H. Sharif and Y. Yang, "An Adaptive Approach to Estimation and Compensation of Frequency-Dependent I/Q Imbalances in MIMO-OFDM Systems," *Proceedings of IEEE Global Communications Conference*, Honolulu, 2009.

[34] A. H. Sayed, Adaptive Filters, Wiley-IEEE Press, New Jersey, 2008.

[35] D. Manolakis, V. K. Ingle and S. M. Kogon, "Statistical and Adaptive Signal Processing: Spectral Estimation, Signal Modeling, Adaptive Filtering and Array Processing," MA: Artech House Publishers, Boston, 2005.

[36] J. G. Proakis, "Digital Communications," 4th edition, Mc-Graw-Hill, New York, 2000.

[37] R. L. Peterson, R. E. Ziemer and D. E. Borth, "Introduction to Spread-Spectrum Communications," 3rd edition, Prentice Hall, New Jersey, 1995.

[38] X. Wang, H. C. Wu, S. Y. Chang, Y. Wu and J. Y. Chouinard, "Efficient Non-Pilot-Aided Channel Length Estimation for Digital Broadcasting Receivers," *IEEE Transactions on Broadcasting*, Vol. 55, No. 3, September 2009, pp. 633-641.

